Published in final edited form as:
J Am Soc Mass Spectrom. 2009 May ; 20(5): 755–762. doi:10.1016/j.jasms.2008.12.022.

A novel Fourier Transform Ion Cyclotron Resonance Mass Spectrometer with improved ion trapping and detection capabilities

Nathan K. Kaiser, **Gunnar E. Skulason**, **Chad R. Weisbrod**, and **James E. Bruce***
Department of Chemistry, Washington State University, Pullman, WA 99164-4630

Abstract

A novel Fourier transform ion cyclotron resonance (FT-ICR) mass spectrometer has been developed for improved biomolecule analysis. A flared metal capillary and an electrodynamic ion funnel were installed in the source region of the instrument for improved ion transmission. The transfer quadrupole is divided into 19 segments, with the capacity for independent control of DC voltage biases for each segment. Restrained Ion Population Transfer, or RIPT, is used to transfer ions from the ion accumulation region to the ICR cell. The RIPT ion guide reduces mass discrimination that occurs due to time-of-flight effects associated with gated trapping. Increasing the number of applied DC bias voltages from 8 to 18 increases the number of ions that are effectively trapped in the ICR cell. The RIPT ion guide with a novel voltage profile applied during ion transfer provides a 3-4-fold increase in the number of ions that are trapped in the ICR cell compared to gated trapping for the same ion accumulation time period. A novel ICR cell was incorporated in the instrument to reduce radial electric field variation for ions with different *z*-axis oscillation amplitudes. With the ICR cell, called Trapping Ring Electrode Cell or TREC, we can tailor the shape of the trapping electric fields to reduce de-phasing of coherent cyclotron motion of an excited ion packet. With TREC, nearly an order of magnitude increase in sensitivity is observed. The performance of the instrument with the combination of RIPT, TREC, flared inlet and ion funnel is presented.

Introduction

Mass spectrometers have become an indispensable tool in the area of proteomics. The desire to understand complex biological systems and analyze lower abundance proteins in the proteome, demands that more accurate and sensitive instruments be developed [1,2]. Fourier transform ion cyclotron resonance FT-ICR [3-5] mass spectrometry offers the highest performance of any type of mass spectrometer in terms of resolution and mass measurement accuracy [6-8]. FT-ICR-MS enables measurement of thousands of components in a complex mixture in a single spectrum [9,10]. The high performance capabilities FT-ICR-MS increase with longer data acquisition periods [11]. However, this performance also depends on the ability to detect an observable signal for the entire data acquisition period. There are a number of factors such as Coulombic interactions of other ion clouds and electric and magnetic field inhomogeneities which cause the observed signal to rapidly decay [12]. To observe ion signals for a period of time, ions need to be confined parallel to the magnetic field by electric fields

*Corresponding Author: James E. Bruce, Present Address: Department of Genome Sciences, 815 Mercer Street, University of Washington, Seattle, Washington 98195, jimbruce@u.washington.edu, (Phone): 509-592-7742, (Fax): 206-685-7301.

[13]. However, many of the factors which are associated with ion cloud de-phasing result from confining ions to a finite space for FT-ICR-MS analysis.

There are a number of advantages resultant from increased magnetic field strength. For example, the data acquisition period decreases linearly for a defined resolution (increased cyclotron frequency) and the upper mass limit and maximum number of ions increase quadratically [14-17]. Also, the number of ions needed for peak coalescence to occur decreases inverse-quadratically with magnetic field strength [18]. These parameters are critical for top-down proteomic experiments [19-21]. There are several idealized electric field qualities such as quadrupolar trapping field and linearized excitation fields which are difficult to achieve simultaneously with a single cell geometry. Typically the attained field quality is a compromise among the desired field parameters [22]. A large number of ICR cell designs have been developed to target one or more of these electric field features [23,24] and the most common ICR cell geometries in use today are designed to emulate infinitely long excitation electrodes [25,26].

With external ionization sources, ions are usually accumulated outside the magnetic field to allow for differential pumping to produce ultra high vacuum (UHV) conditions required for FT-ICR analysis. Accumulation of ions external to the ICR cell has been shown to increase sensitivity and duty cycle [27]. With external ion accumulation, some form of gated trapping is typically utilized to trap ions within the ICR cell [28,29]. Since regions of electric field inhomogeneities increase inside the ICR cell with larger trapping potentials, it is advantageous to perform FT-ICR measurements at low trapping potentials [30-32]. However, with gated trapping, ions trapped in the ICR cell will have a distribution of kinetic energies along the *z*-axis, which leads to differences in trapping oscillation amplitude [28,33]. Lowering the trap plate potentials below the threshold of *z*-axis kinetic energy of the trapped ions will result in a loss of ions from the ICR cell and a decrease in sensitivity [34]. Therefore, to reach low trapping potentials, ions can be cooled by introducing a pulse of gas into the UHV region or a slow reduction of trapping potential [35]. The addition of a collision gas causes expansion of the magnetron radius. Thus, it is desirable to perform quadrupole axialization which converts magnetron motion to cyclotron motion which is rapidly damped in the presence of a collision gas [36,37]. Although, quadrupolar axialization can also heat the ions translationally, this type of axiallization becomes less critical with higher field magnets since the higher field helps to confine the ions near the *z*-axis. However, these ion cooling and axialization techniques require additional time and are not typically combined on an LC time-scale which requires a high duty cycle. In addition, there is a loss of sensitivity when performing gated trapping in the sense that all ions trapped in the accumulation region are not retrapped at the ICR cell. Also, all ions do not exit the accumulation region at the same time, and ions with different *m*/*z* values reach the ICR cell at different times due to different flight velocities. The ions can be forced out of the accumulation region over a shorter period of time by putting angled wires between the multipoles of the accumulation cell to induce a voltage gradient within the accumulation region [38]. However, mass discrimination due to time-of-flight separation of ions remains problematic [39]. A number of different approaches have also been taken to compensate for time-of-flight separations [40,41].

Commercial FT-ICR mass spectrometer vendors have developed hybrid FT-ICR instruments which have a mass-selective device exterior to the magnetic field. This allows for ion isolation, accumulation, and fragmentation exterior to the ICR cell [42,43]. This has greatly increased the speed and flexibility of the type of experiments that can be performed. Though the instrument described here currently does not have a mass selective device exterior to the ICR cell, our goal was to modify instrument configurations to improve the overall FT-ICR mass spectrometer performance. In this paper, we present a novel FT-ICR mass spectrometer which is designed to overcome some of the weaknesses in current instrument designs. The instrument

incorporates a heated flared metal inlet capillary [44,45] followed by an electrodynamic ion funnel [46,47] for improved ion transmission from atmospheric pressure through the first vacuum stage. A novel quadrupole ion guide called Restrained Ion Population Transfer, or RIPT following the ion accumulation region, is designed to minimize time-of-flight effects during ion transfer to the ICR cell [48]. Finally, a novel ICR cell called Trapping Ring Electrode Cell, or TREC has been developed for minimized ion cloud de-phasing [49].

Experimental

The custom built FT-ICR mass spectrometer described herein utilizes a passively shielded 3 tesla (3T) superconducting magnet with a 160 mm diameter horizontal bore (Magnex Scientific, Abingdon, UK). The vacuum system layout shown in Figure 1A was designed to allow for atmospheric pressure ionization sources such as electrospray ionization to be used. Ions were created through electrospray by applying 2.25 kV to a metal union located before the spray tip. The spray solution for all analytical standards purchased from Sigma (St. Louis, MO) was 49:49:2, by volume, water:methanol:acetic acid. Infusion of the electrospray solution was performed with a syringe pump (Cole-Parmer, Vernon Hills, IL) and maintained at a flow rate of 1μL/min for comparison purposes. Ions enter the mass spectrometer through a 30.5 cm long flared metal capillary (I.D. 0.51 mm) (Small Parts, Miami Lakes, FL). The capillary is held in place by a heating block that is heated to 130°C using two cartridge heaters (Omega Engineering, Stamford, CT). The first vacuum stage was maintained at a pressure of 1.2 – 2.0 Torr with a rough pump. A schematic is shown of the ion optics in Figure 1B. An ion funnel is used to transfer ions through the first pumping stage. A leak valve to atmosphere was added to the first pumping stage to control the pressure for optimized ion transmission through the ion funnel. The ion funnel has 22 electrodes with outer diameter of 35.5 mm and thickness 1.6 mm, with 1.0 mm thick nylon washers used as spacers between the electrodes. The inner diameter of the first electrode was 20.3 mm, the inner diameter of the electrodes decreased linearly with the last electrode having an inner diameter of 2.2 mm. The conductance limit after the ion funnel is 3.0 mm. The RF voltage applied to the ion funnel was ~200 V_{p-p} at 760 kHz. All RF voltages were produced with locally built RF generators. The DC voltage gradient of the ion funnel was set up by applying 150 V to the first electrode and 35 V to the last electrode. The second vacuum stage, located between the conductance limit at the end of the ion funnel and a skimmer, is pumped by the auxiliary port on the molecular drag pump used to pump the third stage. Ions are accumulated in the third pumping stage in a 35.6 cm long quadrupole operated with an RF voltage of 280 V_{p-p} at 1.03 MHz (7.9×10^{-3} Torr). A conductance limit of 2 mm separates the ion accumulation region from the RIPT ion guide. Ions can be accumulated in the third vacuum stage by applying a DC voltage to the conductance limit (~10 V). A UHV gate valve (HVA, Reno, NV) was added between the third and fourth stage of pumping. The source region of the instrument has a *z*-axis translational UHV bellows (McAllister Technical Services, Coeur D'Alene, ID). This allows the source region to be accessed for modification or cleaning while still maintaining the UHV needed for FT-ICR-MS analysis. The pressure on the high vacuum side of the gate valve (1×10^{-5} Torr) is monitored with a Micro-Ion gauge (Granville-Phillips, Longmont, CO). The ion transfer technique called restrained ion population transfer, or RIPT, has been described in detail elsewhere [48]. Briefly, the ion guide consists of a 155 cm long quadrupole that has been divided into 19 individual quadrupole segments, with each segment 7.62 cm in length. The segmented quadrupole allows for independent control over DC potentials applied to each segment. The pressure in the UHV region of the instrument was 2×10^{-9} Torr, monitored with a Stable-Ion gauge (Granville-Phillips, Longmont, CO). All metallic vacuum chamber components that extend into the bore of the superconducting magnet were fabricated out of titanium, chosen for its non-magnetic properties. The final vacuum stage was evacuated by a Cryo-Torr 8 Cryopump (Helix Technology, Mansfield, MA) with a custom designed cyropanel which is shown in Figure 1C. The cryopumping surface, fabricated locally, was based on a similar design developed at

Pacific Northwest National Laboratory (Richland, WA) [35]. The original radiative shield and cryopumping surface was replaced with a design that consisted of two concentric cylinders that extend into the bore of the magnet. The outer tube that acted as a radiative heat shield was fabricated from 10.16 cm O.D. × 1.59 mm thick 6061 aluminum with a total tube length of 77.5 cm. The inner cylinder which connected to the cold finger of the cyropump, was fabricated from a 1.59 mm thick sheet of OFHC copper rolled into a cylinder with an O.D. of 6.67 cm. The length of the inner copper cylinder was 73.6 cm. The outer radiative shield was cooled to 80 K and the cyropumping surface was cooled to 13 K. This design provided a maximum pumping speed calculated to be ~4×10^4 L/s for air based on the surface area of the cryopanel. This cryopump replaces a molecular turbopump (400 L/s) which maintained a working pressure of 4×10^{-9} Torr in the final vacuum stage, with the addition of two conductance limits. This design allowed us to remove the conductance limits within the ion guide while maintaining the partitions between vacuum stages. The measured pressure in the final vacuum stage was 2×10^{-9} Torr and provides increased pumping near the ICR cell where ion detection takes place.

The instrument incorporates a novel ICR cell (Trapping Ring Electrode Cell, or TREC), which is a closed cylindrical cell (4.76 cm dia. × 5.08 cm length) with 5 concentric rings replacing the conventional solid trapping electrodes. Individual voltages applied to each of the ring electrodes are designed to create electric fields which minimize differences in radial force at different *z*-axis amplitudes. The Inoue and Gross groups have introduced similar cell designs for segmentation of the end cap electrodes [50,51]. The design of the cell is described in detail elsewhere [46]. The ICR cell is mounted to a titanium flange on the back end of the vacuum system. The preamplifier was supplied by Pacific Northwest National Laboratory. Data were collected with a modular FT-ICR-MS data station (MIDAS) supplied by the National High Magnetic Field Laboratory at Florida State University [52]. Ions were excited with broadband frequency-sweep excitation, with a sweep width of 240 kHz. The sweep rate and excitation amplitude were varied to change the excited cyclotron radius. The excitation waveform created by the arbitrary waveform generator was amplified by a novel RF excitation amplifier developed locally (Skulason, G.E., Bruce, J.E., manuscript in preparation). ICR-2LS software package was used for all data analysis [53].

Results and Discussion

Many challenges associated with high performance signal acquisition with FT-ICR mass spectrometers such as ion cloud de-phasing, space charge frequency shifts, and Coulombic interaction of ion packets are amplified at low magnetic field strength; although these problems persist at higher magnetic field strength, they are not as detrimental to accurate mass analysis. FT-ICR mass spectrometers that have low field magnets, such as the 3T instrument described here, are not in routine use for biological applications because of the disadvantages already mentioned. However, identifying the source of these limitations and developing methods to minimize them can be done without investing in a higher field magnet. The performance gains demonstrated on our 3T mass spectrometer will also translate into increased performance with instruments which incorporate higher field magnets.

Ion transfer

To minimize time-of-flight effects, a ramped voltage bias profile is applied separately to each of the quadrupole segments. This novel voltage scheme allows ions to be moved from the accumulation region to the ICR cell while maintaining complete axial containment. The pulse sequence for a typical ion transfer is shown in Figure 2. Here, ions were trapped in the accumulation quadrupole for 50 ms by applying +10 volts to the front conductance limit. Ions enter the RIPT ion guide when the voltage applied to the front conductance limit was lowered. After 20 ms the voltage to the front conductance limit was restored to a high value to prevent

additional ions from entering the ion guide. The voltage ramp sequence for each adjacent segment was delayed by 8.5 ms. This delay was chosen so that four quadruople segments composed the bottom of the voltage well, which is approximately equal to the length of the accumulation quadrupole. The voltage well moves along the ion guide by simultaneously decreasing the voltage applied to the leading segments and increasing the voltage applied to the trailing segments. By maintaining the same ion trapping dimensions, there is minimal change in space charge in the ion guide during transfer. However, the last electrode in the ion guide is held at +10 V. When the last quadrupole segment reaches a low value the ions become trapped between a preceding segment and an exit electrode. The length of the voltage well decreases to just one segment as the voltage to the preceding segments increases. This compresses the trapped ions into a smaller region similar in length to the ICR cell. When the voltage applied to the last segment is dropped for 0.15 ms, ions are injected into the ICR cell. Compressing the trapped ions to a smaller region before injection into the ICR cell increases the number of ions that are trapped at the ICR cell.

In our initial studies with the RIPT ion guide, the number of possible DC bias voltages were limited to eight by software and hardware that were available at that time [48]. Although the ion guide was constructed with 19 segments, only 8 DC bias potentials could be applied. Therefore, adjacent segments received the same DC bias potential. Thus, the length of the trapping well was larger and, with limited number of DC bias voltages available, it was not possible to compress the ions before transfer to the ICR cell. Although an improved mass range was observed compared to gated trapping with this setup; it suffered from a reduction in signal magnitude. Modification to the software program and the addition of new hardware made it possible to increase the number of possible DC bias potentials to allow each of the segments to have its own DC bias potential. Figure 3A illustrates which segments received the same DC bias for different numbers of total DC bias voltages. Figure 3B illustrates the combined signal magnitude observed for a broadband spectrum of ubiquitin when different numbers of applied DC potentials are used to transfer ions. Each data point is an average of three data acquisitions, with each acquisition an average of 10 scans. Increasing the number of individually-biased segments effectively increases the number of ions that are trapped in the ICR cell, which is reflected in the total signal magnitude in the spectrum. By increasing the number of segments, the length of the trapping region remains more consistent throughout the transfer process. Also, right before ion injection into the ICR cell, the length of the voltage well is reduced from a length approximately equal to accumulation quadrupole to a length of the ICR cell. These results further suggest that the addition of still more segments would further improve the ion transmission performance.

The RIPT method can be compared directly to gated trapping by applying the same DC bias to all the segments. In this mode of operation, the RIPT ion guide transmits ions with the same efficiency as a solid set of quadrupole rods. The direct comparison between the two transfer methods by direct infusion of 1μM BSA digest is shown in Figure 4, all other parameters were the same between the two experiments. The same ion accumulation time period of 300 ms is used for both transfer methods. In the mass spectrum collected with the RIPT method, the overall observed ion magnitude increased approximately 3-fold compared to that observed with gated trapping. We were also able to detect twice as many isotopic distributions when ions were transferred with the RIPT method. The total ion transfer time with RIPT was ~300 ms compared to 2.8 ms for gated trapping. However, to achieve the same detected ion signal with gated trapping as with RIPT, we would need to increase the ion accumulation time period 3 fold. Although the RIPT process decreases the overall duty cycle for a set ion accumulation time period, it can actually increase the duty cycle for a set number of ions. Also, it is possible to transfer multiple ion packets simultaneously through the ion guide. Thus, while one ion packet is being analyzed in the ICR cell another is being transferred through the ion guide, which results in a further increase in the duty cycle.

Ion detection

The sensitivity of the instrument was tested in two different modes, 1) applying the same voltage to all trapping rings during detection (common) and 2) applying a separate voltage to each trapping ring during detection (TREC). By applying a common voltage to each of the rings, the electric field within the trapping region of the ICR cell is the same as if a single solid electrode was used. This allows for a direct comparison between a closed ICR cell and TREC. By applying separate voltages to each of the rings, the electric fields within the trapping region of the ICR cell are modified. The voltages are applied so that the outward directed force from the electric fields is constant along the *z*-axis of the ICR cell. A serial dilution of melittin was used to test the limits of detection for ions transferred to the ICR cell with the RIPT transfer method. To minimize effects from contamination from carryover, the sample with the lowest concentration was run first. The results from the serial dilution are shown as a stacked plot with the melittin $(M+4H)^{4+}$ ion in Figure 5A. The length of the ion accumulation time period was adjusted for different concentrations of analyte. All of the spectra were collected as single data acquisitions. Signal averaging would further improve the limit of detection of the instrument. With the exception of changing trapping voltages before detection, all other instrument parameters were held constant between the normal mode and TREC. With TREC, there is nearly an order of magnitude increase in sensitivity compared to the normal operation mode. The ratio of signal magnitude between normal and TREC at each of the sample concentrations is shown in Figure 5B. These data illustrate that the improvement in signal magnitude with TREC is constant at all concentrations. The improvement in sensitivity at low concentrations suggests that switching the applied trapping voltages between excitation and detection does not destabilize the coherent cyclotron motion of the ion cloud, even for a very low number of ions.

The combination of RIPT and TREC is compared to gated trapping and common voltages applied to all ring electrodes. The complexity of ion motion inside the ICR cell becomes more intricate with a larger number of ion packets present due to Coulombic interactions. Therefore, infusion of a complex mixture is used to test instrument performance. Analysis of a complex mixture becomes more challenging at lower magnetic field strength due to more profound space charge frequency shifts and decreased cyclotron frequency. Thus, to minimize space charge variation one can either work with a lower number of ions or excite ions to a large cyclotron radius. Figure 6 illustrates the improvement when operating the instrument with the combination of RIPT and TREC with direct infusion of 1μM BSA tryptic digest. With TREC, we are able to excite ions to a larger cyclotron radius while minimizing electric field inhomogeneity [49]. Thus, we are able to observe ion signal for a longer period of time. Also, at larger cyclotron radius the Coulombic interaction of other ion packets are reduced. With common voltages applied to all the ring electrodes, increasing the excited cyclotron radius reduced the length of observed signal due to increased electric field inhomogeneity. Increasing the number of ions decreased the detectable signal duration of lower abundance species likely due to increased Coulombic interactions. The average mass measurement accuracy with external calibration for the gated-common experiment is 3.16 ppm (19 identified peptides); this is decreased to 2.16 ppm (28 identified peptides) for the RIPT-TREC experiment. The search window was 10 ppm. The distribution of mass measurement errors is shown in a histogram.

Conclusions

A novel FT-ICR mass spectrometer with a 3 tesla magnet has been designed and initial performance described. This instrument has a transfer quadrupole ion guide that has been divided into 19 segments for control of the axial position of the trapped ions throughout the entire transfer process, which effectively eliminates time of flight mass discrimination. We

show that with this transfer methodology ions are transmitted more effectively to the ICR cell compared to gated trapping, indicated by increased signal magnitude. Increasing the number of quadrupole segments from our initial report increases the transfer efficiency through the device. Our results indicate that a further increase in the number of segments is needed for optimization of the transfer technique.

Modulating the voltage applied to each of the ring electrodes with TREC allows ions to have more stable ion motion at larger cyclotron radii, which is important since exciting ions to larger cyclotron radii will increase sensitivity as well as the signal-to-noise ratio. Use of TREC allows ions to be excited to larger cyclotron radii by reducing electric field inhomogeneity. TREC offers a 4-fold improvement in signal magnitude compared to the same voltage applied to all ring electrodes. We demonstrate with a combination of the RIPT transfer method with the TREC ICR cell an increase in the number of identified peptides with greater mass measurement accuracy compared to gated trapping with a closed ICR cell. With sensitivity, dynamic range and mass measurement accuracy the most challenging aspects of proteomics research, the developments illustrated above suggest improved capabilities for protein identification can be achieved through novel cell, ion guide and source design.

Acknowledgments

We thank the National High Magnetic Field Laboratory for the use of their MIDAS data station to carry out FT-ICR MS experiments. This material is based upon work supported by the National Science Foundation under Grant No. 0352451; Murdock Charitable Trust; Office of Science (BER), U. S. Department of Energy, Grant No. DE-FG02-04ER63924, and the National Institutes of Health Biotechnology Training Grant.

References Cited

1. He F, Emmett MR, Hakansson K, Hendrickson CL, Marshall AG. Theoretical and experimental prospects for protein identification based solely on accurate mass measurement. Journal of Proteome Research 2004;3:61–67. [PubMed: 14998164]
2. Clauser KR, Baker P, Burlingame AL. Role of Accurate Mass Measurement (+-10 ppm) in Protein Identification Strategies Employing MS or MS/MS and Database Searching. Analytical Chemistry 1999;71:2871–2882. [PubMed: 10424174]
3. Comisarow MB, Marshall AG. Fourier transform ion cyclotron resonance spectroscopy. Chemical Physics Letters 1974;25:282–283.
4. Comisarow MB, Marshall AG. Frequency-sweep Fourier transform ion cyclotron resonance spectroscopy. Chemical Physics Letters 1974;26:489–490.
5. Amster IJ. Fourier transform mass spectrometry. Journal of Mass Spectrometry 1996;31:1325–1337.
6. He F, Hendrickson CL, Marshall AG. Baseline mass resolution of peptide isobars: A record for molecular mass resolution. Analytical Chemistry 2001;73:647–650. [PubMed: 11217775]
7. Williams DK Jr, Muddiman DC. Parts-Per-Billion Mass Measurement Accuracy Achieved through the Combination of Multiple Linear Regression and Automatic Gain Control in a Fourier Transform Ion Cyclotron Resonance Mass Spectrometer. Analytical Chemistry 2007;79:5058–5063. [PubMed: 17539605]
8. Shi SDH, Hendrickson CL, Marshall AG. Counting individual sulfur atoms in a protein by ultrahigh-resolution Fourier transform ion cyclotron resonance mass spectrometry: experimental resolution of isotopic fine structure in proteins. Proceedings of the National Academy of Sciences U S A 1998;95:11532–11537.
9. McLafferty FW, Fridriksson EK, Horn DM, Lewis MA, Zubarev RA. Techview: biochemistry. Biomolecule mass spectrometry. Science 1999;284:1289–1290. [PubMed: 10383309]
10. Hughey CA, Rodgers RP, Marshall AG. Resolution of 11,000 Compositionally Distinct Components in a Single Electrospray Ionization Fourier Transform Ion Cyclotron Resonance Mass Spectrum of Crude Oil. Analytical Chemistry 2002;74:4145–4149. [PubMed: 12199586]

11. Marshall AG, Hendrickson CL. Fourier transform ion cyclotron resonance detection: principles and experimental configurations. International Journal of Mass Spectrometry 2002;215:59–75.
12. Peurrung AJ, Kouzes RT. Long-term coherence of the cyclotron mode in a trapped ion cloud. Physical Review. E. Statistical Physics, Plasmas, Fluids, and Related Interdisciplinary Topics 1994;49:4362–4368.
13. McIver RT Jr, Ledford EB Jr, Miller JS. Proposed method for mass spectrometric analysis for ultra-low vapor pressure compounds. Analytical Chemistry 1975;47:692–697.
14. Mitchell DW. Realistic simulation of the ion cyclotron resonance mass spectrometer using a distributed three-dimensional particle-in-cell code. Journal of the American Society for Mass Spectrometry 1999;10:136–152.
15. Mitchell DW, Smith RD. Prediction of a space charge induced upper molecular mass limit towards achieving unit mass resolution in Fourier transform ion cyclotron resonance mass spectrometry. Journal of Mass Spectrometry 1996;31:771–790.
16. Marshall AG, Guan S. Advantages of high magnetic field for Fourier transform ion cyclotron resonance mass spectrometry. Rapid Communications in Mass Spectrometry 1996;10:1819–1823.
17. Schaub TM, Hendrickson CL, Horning S, Quinn JP, Senko MW, Marshall AG. High-Performance Mass Spectrometry: Fourier Transform Ion Cyclotron Resonance at 14.5 Tesla. Analytical Chemistry (Washington, DC, United States) 2008;80:3985–3990.
18. Mitchell DW, Smith RD. Cyclotron motion of two Coulombically interacting ion clouds with implications to Fourier-transform ion cyclotron resonance mass spectrometry. Physical Review. E. Statistical Physics, Plasmas, Fluids, and Related Interdisciplinary Topics 1995;52:4366–4386.
19. Bogdanov B, Smith RD. Proteomics by FTICR mass spectrometry: Top down and bottom up. Mass Spectrometry Reviews 2005;24:168–200. [PubMed: 15389855]
20. Kelleher NL, Lin HY, Valaskovic GA, Aaserud DJ, Fridriksson EK, McLafferty FW. Top Down versus Bottom Up Protein Characterization by Tandem High-Resolution Mass Spectrometry. Journal of the American Chemical Society 1999;121:806–812.
21. Sze SK, Ge Y, Oh H, McLafferty FW. Top-down mass spectrometry of a 29-kDa protein for characterization of any posttranslational modification to within one residue. Proceedings of the National Academy of Sciences U S A 2002;99:1774–1779.
22. Guan S, Marshall AG. Ion traps for Fourier transform ion cyclotron resonance mass spectrometry: principles and design of geometric and electric configurations. International Journal of Mass Spectrometry and Ion Processes 1995;146/147:261–296.
23. Anderson JS, Vartanian H, Laude DA. Evolution of trapped ion cells in Fourier transform ion cyclotron resonance mass spectrometry. Trends Anal Chem 1994;13:234–239.
24. Vartanian VH, Anderson JS, Laude DA. Advances in trapped ion cells for Fourier transform ion cyclotron resonance mass spectrometry. Mass Spectrometry Reviews 1995;14:1–19.
25. Caravatti P, Allemann M. The infinity cell: a new trapped-ion cell with radiofrequency covered trapping electrodes for Fourier transform ion cyclotron resonance mass spectrometry. Organic Mass Spectrometry 1991;26:514–518.
26. Beu SC, Laude DA Jr. Elimination of axial ejection during excitation with a capacitively coupled open trapped-ion cell for Fourier transform ion cyclotron resonance mass spectrometry. Analytical Chemistry 1992;64:177–180.
27. Senko MW, Hendrickson CL, Emmett MR, Shi SDH, Marshall AG. External accumulation of ions for enhanced electrospray ionization Fourier transform ion cyclotron resonance mass spectrometry. Journal of the American Society for Mass Spectrometry 1997;8:970–976.
28. Gorshkov MV, Masselon CD, Anderson GA, Udseth HR, Harkewicz R, Smith RD. A dynamic ion cooling technique for FTICR mass spectrometry. Journal of the American Society for Mass Spectrometry 2001;12:1169–1173. [PubMed: 11720391]
29. Caravatti, P. US Patent. 4,924,089. 1990.
30. Easterling ML, Pitsenberger CC, Kulkarni SS, Taylor PK, Amster IJ. A 4.7 Tesla internal MALDI-FTICR instrument for high mass studies: performance and methods. International Journal of Mass Spectrometry and Ion Processes 1996;157/158:97–113.

31. Stults JT. Minimizing peak coalescence: high-resolution separation of isotope peaks in partially deamidated peptides by matrix-assisted laser desorption/ionization Fourier transform ion cyclotron resonance mass spectrometry. Analytical Chemistry 1997;69:1815–1819.
32. Solouki T, Emmett MR, Guan S, Marshall AG. Detection, number and sequence location of sulfur-containing amino acids and disulfide bridges in peptides by ultrahigh-resolution MALDI FTICR mass spectrometry. Analytical Chemistry 1997;69:1163–1168. [PubMed: 9075406]
33. Nikolaev EN, Miluchihin N, Inoue M. Evolution of an ion cloud in a Fourier transform ion cyclotron resonance mass spectrometer during signal detection: its influence on spectral line shape and position. International Journal of Mass Spectrometry and Ion Processes 1995;148:145–157.
34. Wong Richard L, Amster IJ. Sub part-per-million mass accuracy by using stepwise-external calibration in fourier transform ion cyclotron resonance mass spectrometry. Journal of the American Society for Mass Spectrometry 2006;17:1681–1691. [PubMed: 16934995]
35. Winger BE, Hofstadler SA, Bruce JE, Udseth HR, Smith RD. High-resolution accurate mass measurements of biomolecules using a new electrospray ionization ion cyclotron resonance mass spectrometer. Journal of the American Society for Mass Spectrometry 1993;4:566–577.
36. Guan S, Kim HS, Marshall AG, Wahl MC, Wood TD, Xiang X. Shrink-wrapping an ion cloud for high-performance Fourier transform ion cyclotron resonance mass spectrometry. Chemical Reviews 1994;94:2161–2182.
37. Guan S, Gorshkov MV, Marshall AG. Circularly polarized quadrature excitation for Fourier-transform ion cyclotron resonance mass spectrometry. Chemical Physics Letters 1992;198:143–148.
38. Wilcox BE, Hendrickson CL, Marshall AG. Improved ion extraction from a linear octopole ion trap: SIMION analysis and experimental demonstration. Journal of the American Society for Mass Spectrometry 2002;13:1304–1312. [PubMed: 12443021]
39. Wong RL, Amster IJ, Combining Low. High Mass Ion Accumulation for Enhancing Shotgun Proteome Analysis by Accurate Mass Measurement. Journal of the American Society for Mass Spectrometry 2006;17:205–212. [PubMed: 16413206]
40. O'Connor PB, Duursma MC, van Rooij GJ, Heeren RMA, Boon JJ. Correction of time-of-flight shifted polymeric molecular weight distributions in matrix-assisted laser desorption/ionization Fourier transform mass spectrometry. Analytical Chemistry 1997;69:2751–2755.
41. Dey M, Castoro JA, Wilkins CL. Determination of Molecular Weight Distributions of Polymers by MALDI-FTMS. Analytical Chemistry 1995;67:1575–1579.
42. Belov ME, Rakov VS, Nikolaev EN, Goshe MB, Anderson GA, Smith RD. Initial implementation of external accumulation liquid chromatography/electrospray ionization Fourier transform ion cyclotron resonance with automated gain control. Rapid Communications in Mass Spectrometry 2003;17:627–636. [PubMed: 12661014]
43. Belov ME, Nikolaev EN, Anderson GA, Udseth HR, Conrads TP, Veenstra TD, Masselon CD, Gorshkov MV, Smith RD. Design and performance of an ESI interface for selective external ion accumulation coupled to a fourier transform ion cyclotron mass spectrometer. Analytical Chemistry 2001;73:253–261. [PubMed: 11199974]
44. Prior, DC.; Price, J.; Bruce, JE. U S Patent 6,455,8646. 2002.
45. Wu S, Zhang K, Kaiser NK, Bruce JE, Prior DC, Anderson GA. Incorporation of a Flared Inlet Capillary Tube on a Fourier Transform Ion Cyclotron Resonance Mass Spectrometer. Journal of the American Society for Mass Spectrometry 2006;17:772–779. [PubMed: 16603374]
46. Shaffer SA, Prior DC, Anderson GA, Udseth HR, Smith RD. An ion funnel interface for improved ion focusing and sensitivity using electrospray ionization mass spectrometry. Analytical Chemistry 1998;70:4111–4119. [PubMed: 9784749]
47. Shaffer SA, Tolmachev A, Prior DC, Anderson GA, Udseth HR, Smith RD. Characterization of an Improved Electrodynamic Ion Funnel Interface for Electrospray Ionization Mass Spectrometry. Analytical Chemistry 1999;71:2957–2964. [PubMed: 10450147]
48. Kaiser NK, Skulason GE, Weisbrod CR, Wu S, Zhang K, Prior DC, Buschbach MA, Anderson GA, Bruce JE. Restrained ion population transfer: a novel ion transfer method for mass spectrometry. Rapid Communications in Mass Spectrometry 2008;22:1–10. [PubMed: 18041795]

49. Weisbrod CR, Kaiser NK, Skulason GE, Bruce JE. Trapping Ring Electrode Cell (TREC): A novel FT-ICR mass spectrometer cell for iproved signal-to-noise and resolving power. Analytical Chemistry. 2008

50. Gooden JK, Rempel DL, Gross ML. Evaluation of different combinations of gated trapping, RF-only mode and trap compensation for in-field MALDI Fourier transform mass spectrometry. J Am Soc Mass Spectrom 2004;15:1109–1115. [PubMed: 15234369]

51. Naito Y, Fujiwara M, Inoue M. Improvement of the electric field in the cylindrical trapped-ion cell. International Journal of Mass Spectrometry and Ion Processes 1992;120:179–192.

52. Senko MW, Canterbury JD, Guan S, Marshall AG. A high-performance modular data system for Fourier transform ion cyclotron resonance mass spectrometry. Rapid Communications in Mass Spectrometry 1996;10:1839–1844. [PubMed: 8953786]

53. Anderson, GA.; Bruce, JE.; Smith, RD. ICR-2LS. Richland, WA: 1996.

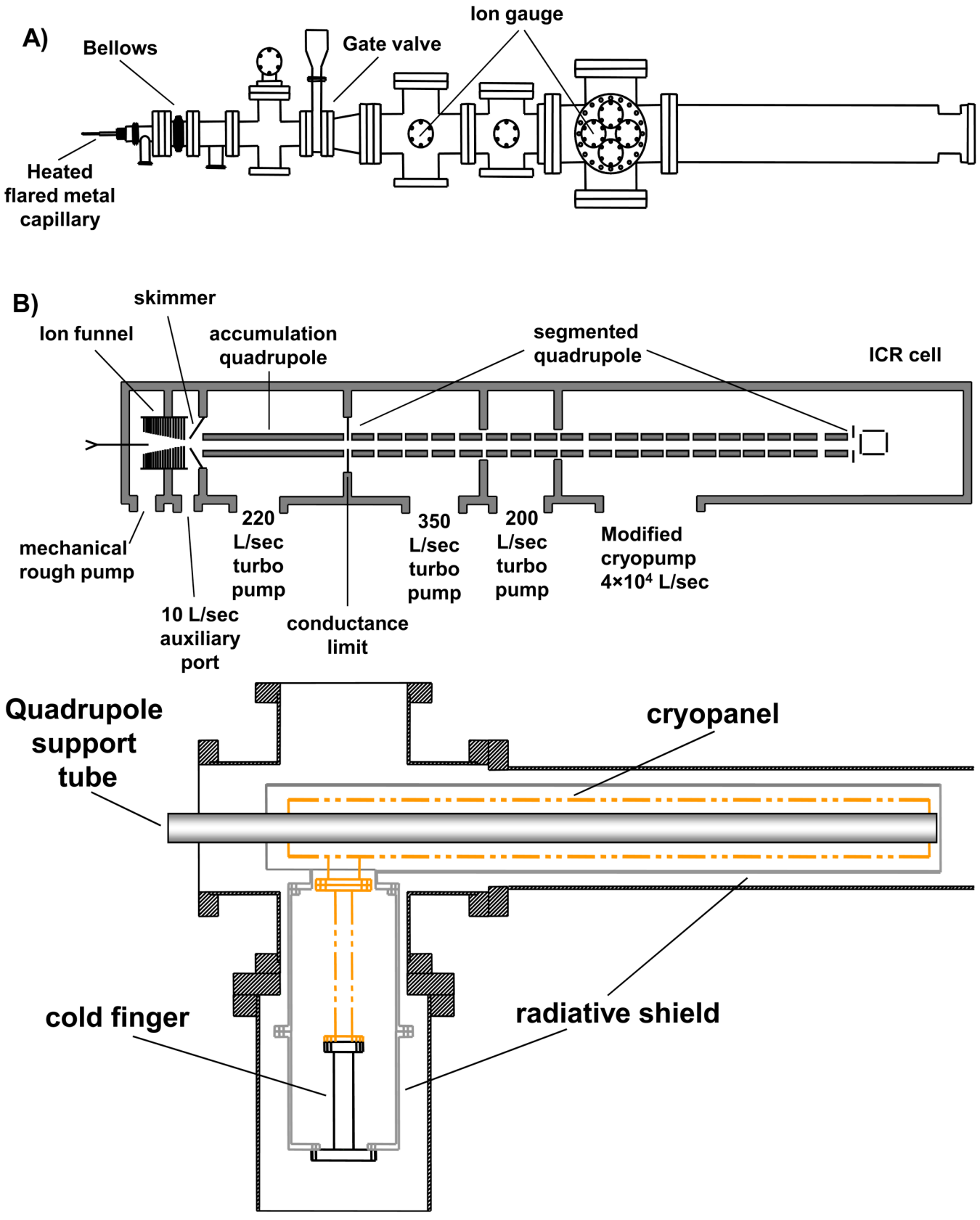

Figure 1.

A) Representation of the vacuum system of the FT-ICR mass spectrometer. B) Schematic representation of the ion transfer electrodes and vacuum pumping configuration. C) A schematic of the modified cryopumping surface installed in the instrument.

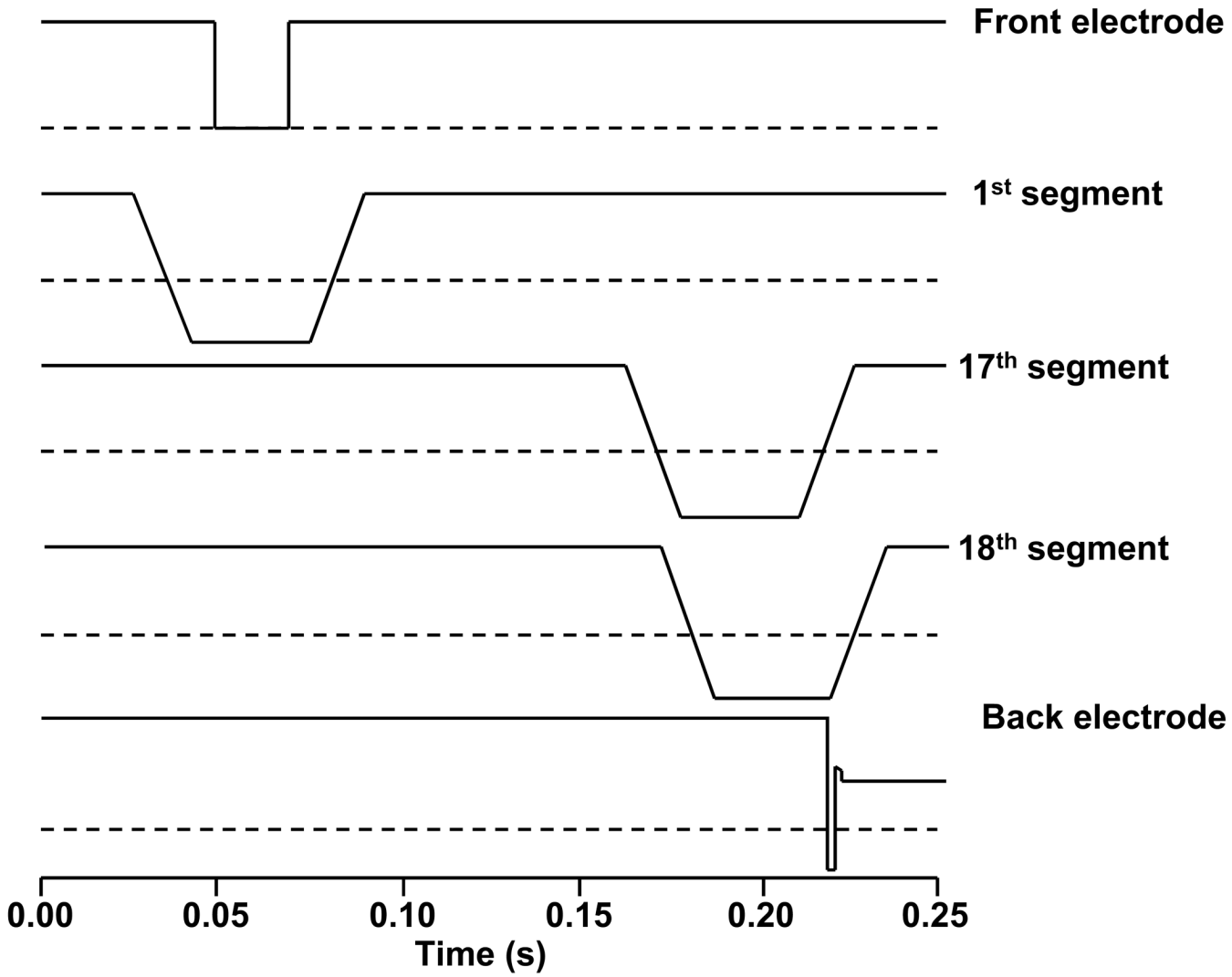

Figure 2.
Voltage profile applied to select ion guide segments during the ion transfer process. The dotted line represents ground in each profile.

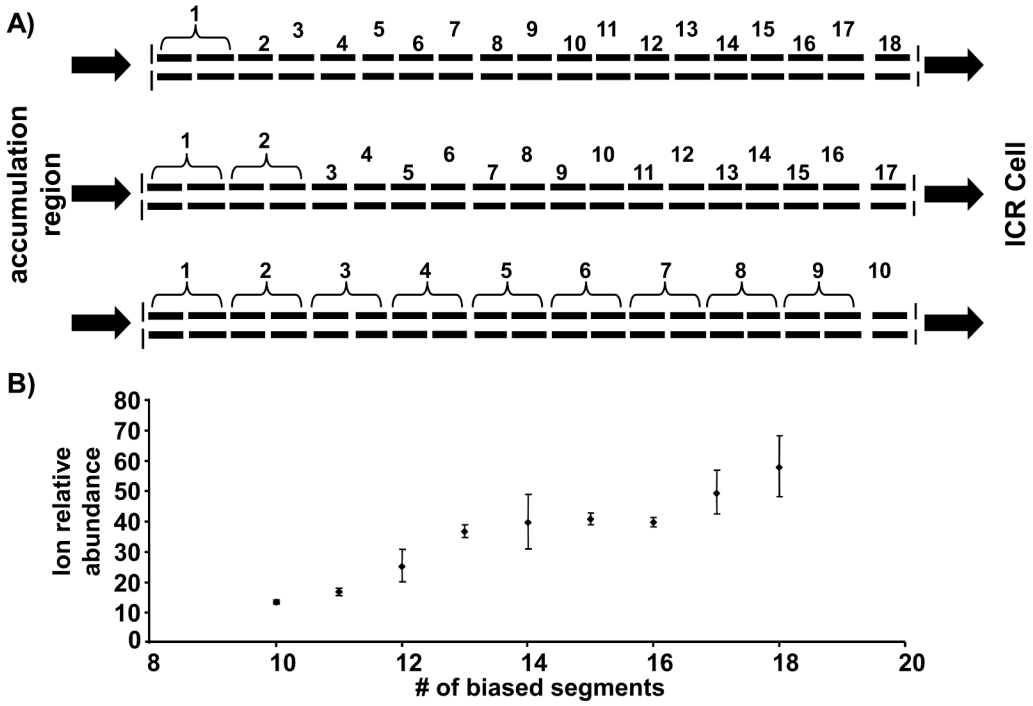

Figure 3.

A) A visual representation of how the segments were coupled together for the different total number of applied DC bias voltages. B) The combined signal magnitude as a function of number of independent DC bias voltages that were applied during the RIPT transfer method. The error bars represent + and - one standard deviation.

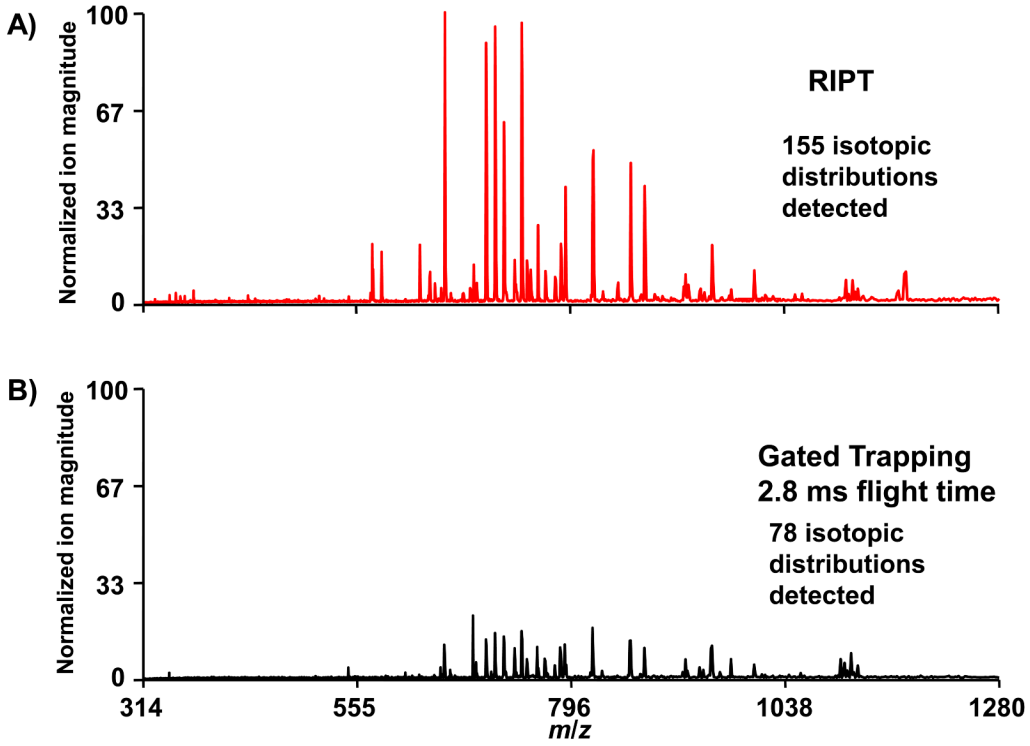

Figure 4.

ESI-FTICR mass spectra taken with the RIPT method (A) and gated trapping with a flight time of 2.8 ms (B) are shown. The y-axes in both spectra are normalized to the most strong peak in the spectrum obtained with the RIPT method. A 3-fold improvement in signal magnitude is observed with the RIPT method for the same ion accumulation time period.

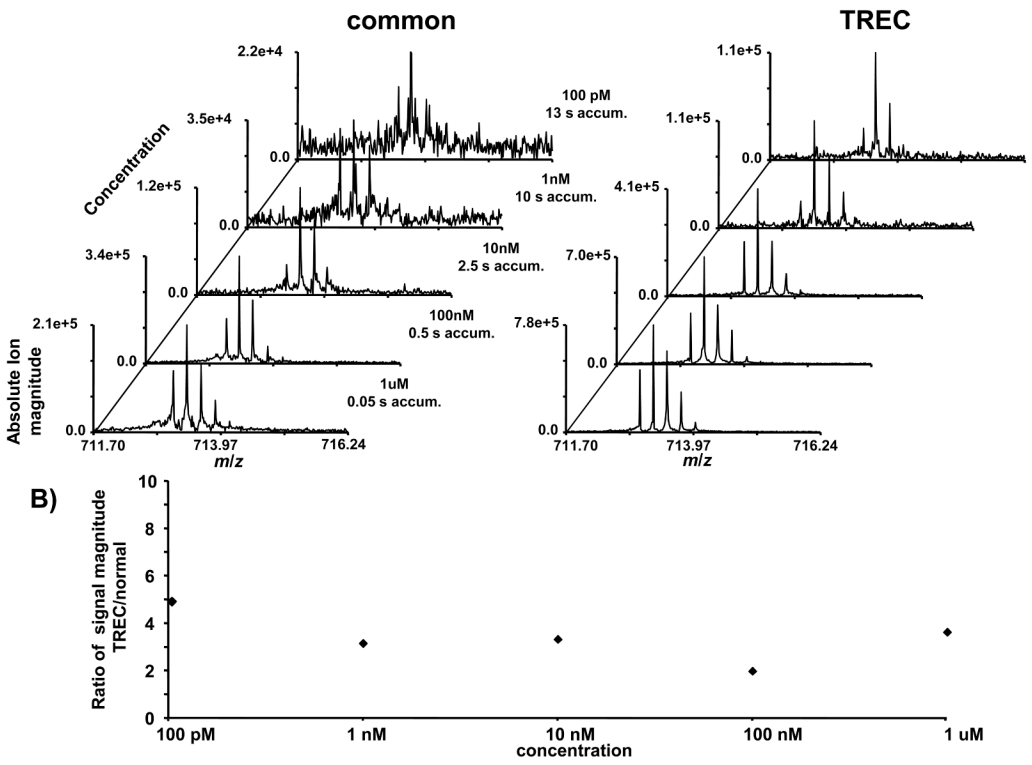

Figure 5.

A) The sensitivity of the instrument is compared between common voltages applied to all trapping rings and TREC. B) The ratio of signal magnitude between TREC and common voltages are shown at different concentrations. The increase in signal magnitude remains constant at different analyte concentrations.

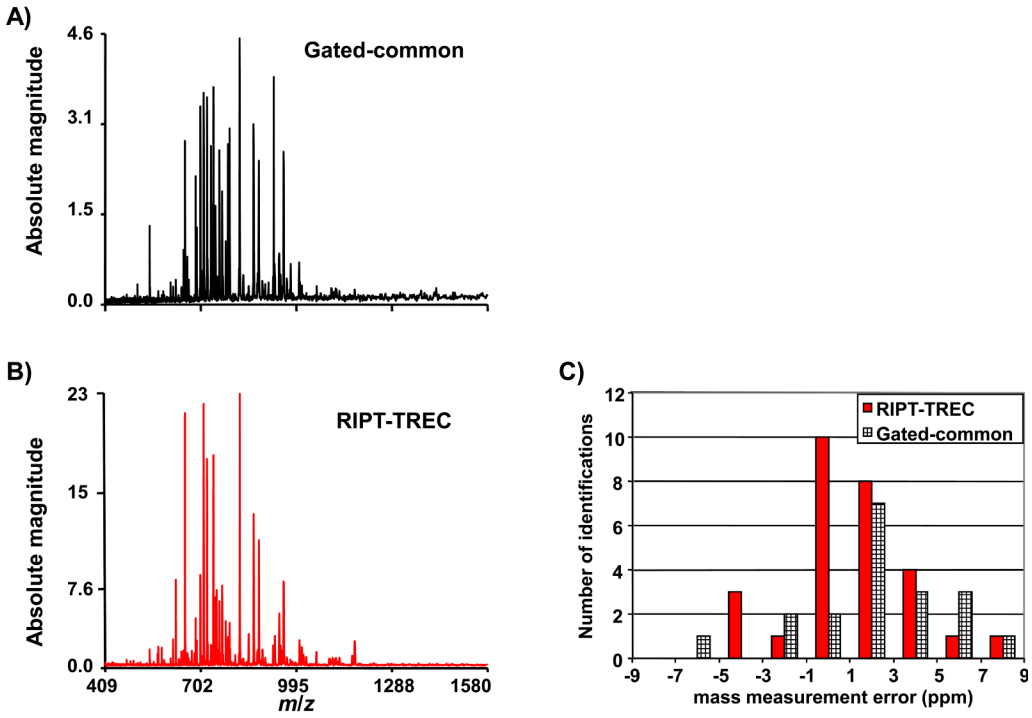

Figure 6.

A comparison of the RIPT-TREC method (A) with gated-common voltages (B) for a complex mixture of BSA tryptic digest. The RIPT-TREC method shows approximately a 5-fold improvement in detected signal magnitude compared to that observed with gated trapping. C) A histogram of the number of peptides identified within the selected mass measurement error bin.